

# KH 15D: Gradual Occultation of a Pre–Main-Sequence Binary

Joshua N. Winn<sup>1,2</sup>, Matthew J. Holman<sup>1</sup>, John A. Johnson<sup>3</sup>,  
Krzysztof Z. Stanek<sup>1</sup>, Peter M. Garnavich<sup>4</sup>

## ABSTRACT

We propose that the extraordinary “winking star” KH 15D is an eccentric pre–main-sequence binary that is gradually being occulted by an opaque screen. This model accounts for the periodicity, depth, duration, and rate of growth of the modern eclipses; the historical light curve from photographic plates; and the existing radial velocity measurements. It also explains the re-brightening events that were previously observed during mid-eclipse, and the subsequent disappearance of these events. We predict the future evolution of the system and its full radial velocity curve. Given the small velocity of the occulting screen relative to the center of mass of the binary, the screen is probably associated with the binary, and may be the edge of a precessing circumbinary disk.

*Subject headings:* stars: pre-main sequence — stars: individual (KH 15D) — circumstellar matter — open clusters and associations: individual (NGC 2264)

## 1. Introduction

While monitoring stars in the young cluster NGC 2264, Kearns & Herbst (1998) noticed that star #15 in field D of their sample had a bizarre and unprecedented light curve. This object, known as KH 15D, undergoes periodic eclipses ( $P = 48.35$  days) that are remarkable for their depth (3.5 mag) and duration (currently  $\approx 24$  days). There is consensus that the eclipses are caused by circumstellar material, but not on the composition or spatial distribution of that material. Previously proposed theories include an edge-on circumstellar disk (Hamilton et al. 2001, Agol et al. 2003, Winn et al. 2003), an orbiting vortex of solid particles (Barge & Viton 2003), and an asymmetric common envelope (Grinin & Tambovtseva 2002).

---

<sup>1</sup>Harvard-Smithsonian Center for Astrophysics, 60 Garden St., Cambridge, MA 02138

<sup>2</sup>National Science Foundation Astronomy & Astrophysics Postdoctoral Fellow

<sup>3</sup>Department of Astronomy, University of California, Berkeley, CA 94720

<sup>4</sup>University of Notre Dame, Notre Dame, IN 46556

The system has attracted the attention of numerous observers because the fortuitous alignment may allow unique studies of circumstellar (or even protoplanetary) processes, and because the occulting edge can be used as a “natural coronagraph” to map out the environment of the underlying T Tauri star (Hamilton et al. 2003, Agol et al. 2003, Deming, Charbonneau, & Harrington 2003). The system is the target of ongoing monitoring campaigns (Herbst et al. 2002) and archival studies (Winn et al. 2003, Johnson & Winn 2003).

In this *Letter* we present the first quantitative model that accounts for all the observed properties of the system. Our main inspiration was the discovery by Johnson & Winn (2003) that in 1970, the eclipses appeared to be diluted by the light of a second star. Building on the demonstration by Herbst et al. (2002) that the ingress and egress light curves can be reproduced by a knife edge crossing the face of a star, we show that the entire historical and modern light curve can be reproduced by a knife edge crossing the mutual orbit of a pair of pre-main-sequence stars. In § 2 we review the peculiar phenomenology of KH 15D and describe how it emerges naturally from the model. In § 3 we determine quantitative fits to the data. Finally, in § 4 we discuss the physical interpretation of the model and predict the results of future investigations into this intriguing system.

## 2. Qualitative description of the model

We would like to understand the following characteristics of KH 15D:

1. Every  $48.35 \pm 0.02$  days, it decreases in brightness from  $I = 14.47$  to  $\approx 18$  (Hamilton et al. 2001 and Herbst et al. 2002, hereafter H01 and H02).
2. The faint state (“eclipse”) currently lasts for approximately half of the photometric period, and the eclipse duration is increasing by about 1 day year<sup>-1</sup> (H02).
3. Near the middle of an eclipse, the flux has been observed to rise and fall abruptly. In 1995-96, these “re-brightenings” briefly returned the system to its uneclipsed flux, or even brighter. Since 1997, the maximum flux during these events has decreased monotonically (H01, H02).
4. Archival observations from 1913 to 1950 are consistent with no eclipses. The system spent  $\lesssim 20\%$  of the time  $>1$  mag fainter than its modern bright state (Winn et al. 2003).
5. Between 1967 and 1982, the system alternated from bright to faint with the same period as observed today, but the fractional variation was much smaller ( $\Delta I = 0.67 \pm 0.07$ ) and

the bright state was  $0.90 \pm 0.15$  magnitude brighter (Johnson & Winn 2003, hereafter JW03).

6. There appears to be a phase shift of  $\approx 180^\circ$  between the 1967-82 light curve and the modern light curve, i.e., the modern bright states have nearly the same phase as the previous faint states (JW03).

All these properties are straightforward consequences of the following model. Consider two stars, A and B, with a projected orbit depicted in Figure 1. An opaque screen with a sharp edge oriented vertically (along the  $y$ -axis) gradually covers the system, moving from left to right (increasing  $x$ ). Whenever the orbital motion of a star carries it to the left of the edge ( $x_{\text{star}} < x_{\text{screen}}$ ), the starlight is blocked.

Before 1960, both stellar orbits were fully exposed, and the flux from the system was time-independent, in compliance with observation #4 of the preceding list. In 1970, the screen covered the left end of B’s orbit, but A remained unobscured. As a result, diluted eclipses of star B were observed (#5). By 2002, the screen covered B’s entire orbit and a significant fraction of A’s orbit, causing today’s periodic, long-lasting, total eclipses (#1). The eclipses grow in duration as the screen continues to advance (#2). The re-brightenings occurred during the time span around 1995, when B’s orbit had not yet been completely covered, allowing B to peek out briefly from behind the screen while A was eclipsed (#3). Because the eclipses in 1970 were of star B, whereas the modern eclipses are of star A, this model produces the phase shift that was tentatively identified by JW03 (#6).

### 3. Quantitative determination of parameters

Rather than directly fitting the model to the voluminous photometric data, we attempted to match the key derived quantities: the eclipse duration in 1967-70, the eclipse duration and its rate of increase from 1997 to 2003, and the ingress and egress durations of 2002 (see Table 1). We also fitted the radial velocity difference of  $3.3 \pm 0.6 \text{ km s}^{-1}$  that Hamilton et al. (2003) measured near the start and end of a particular eclipse in 2001.

We assumed the orbital period is  $P = 48.35$  days and star A has mass  $0.6M_\odot$  and radius  $1.3R_\odot$  (H01). The orbit was specified by the mass ratio, eccentricity, and sequential rotations  $\theta_z$ ,  $\theta_y$ , and  $\theta_x$  about the Cartesian axes defined in Figure 1. The reason for using Cartesian axes rather than traditional orbital elements is to capitalize on certain degeneracies of the model. Rotation about the  $x$ -axis does not affect the light curve. Rotation about the  $y$ -axis affects the projected size of the orbits, but does not affect the projected size of the (spherical) stellar surfaces. Thus,  $\theta_y$  controls the time scale for changes in eclipse duration

relative to the time scales of partial-eclipse phenomena: ingress, egress, and the vanishing of the re-brightening events.

For a given orbit, we produced a model light curve as follows. The speed of the occulting edge relative to the center of mass was determined by requiring the edge to cross B’s orbit between 1963 and 1997. We computed the screen position and the Keplerian orbital position of each star with a time sampling of  $P/100$ . We assumed  $L_B/L_A = 1.0$  (see § 4) and added a time-independent flux of  $0.04L_A$  to represent scattered light (H01, Agol et al. 2003). Whenever  $x_{\text{star}} < x_{\text{screen}} - R_{\text{star}}$ , that star made no contribution to the light curve. When the screen covered only part of a stellar surface, we used the same limb-darkening law as H02 ( $\mu = 0.3$ ) to compute the flux from that star.

First, we optimized  $M_B$ ,  $e$  and  $\theta_z$ , by fitting the eclipse durations and the ratio of durations of ingress and egress. We searched a 3-d grid of models with  $0.5 < M_B/M_A < 2.0$ ,  $0.05 < e < 0.95$ , and  $-90^\circ < \theta_z < 90^\circ$ . The best-fitting solution had  $\chi^2/N_{\text{D.O.F.}} = 0.7$ . Next, we adjusted  $\theta_y$  to increase the ingress and egress durations to the observed values. Due to symmetry, there were two solutions for  $\theta_y$ , differing only in sign. We refer to these as Model 1 and Model 2. For each model, we forced agreement with the radial velocity measurements by tuning  $\theta_x$  and the heliocentric radial velocity of the center of mass. Finally, the radius of star B was tailored to match the ingress and egress durations in 1967-70, and the time scale over which the re-brightening events decreased in intensity.

The parameters of Models 1 and 2, after translating into traditional orbital elements, are given in Table 2. These models produce identical light curves, but have different three-dimensional orbits and radial velocity curves. In addition, there are two solutions not listed in Table 1 that are obtained by reflecting Models 1 and 2 in the  $xz$ -plane. The orbit of Model 1 is depicted in Figure 1. Figure 2 shows the time evolution of eclipse durations and ingress/egress ratio. Figure 3 compares the model light curve with the historical light curves of JW03. The agreement is excellent within the overall uncertainties in zero point and orbital phase of the historical data. Figure 4 illustrates the disappearance of the re-brightenings between 1995 and 1998, and compares the model with the 2001-02 light curve. Figure 5 shows the two possible solutions for the radial velocity curve.

## 4. Discussion

We have shown it is possible to find reasonable stellar and orbital parameters that bring the model into quantitative agreement with the modern and historical light curves, and the available radial velocity data. Certainly we do not claim that our model parameters are

exactly correct. The fitted parameters are subject to our assumptions about the mass and radius of star A, the year that eclipses of star B began, and the constancy of the screen speed, among other things. Nevertheless, we can use the generic properties of the model to make some inferences and predictions about the system.

The speed of the screen relative to the center of mass of the binary is only  $v_x = 13 \text{ m s}^{-1}$ , a scale set by the  $\approx 35$  year crossing time of star B’s projected orbit. This speed seems too small for the screen to be an unrelated foreground phenomenon such as a molecular cloud or bow shock. The screen is probably physically associated with the binary, as also suggested by the small angle between the screen’s edge and the orbital plane of the binary. A circular orbit with speed  $13 \text{ m s}^{-1}$  around a total mass of  $1.0M_\odot$  would have a radius of 25 parsecs, which is too large to remain bound to the system. The speed must represent a phenomenon slower than orbital motion, such as orbital precession.

Hence our hypothesis is that the screen is a precessing circumbinary disk. As a feasibility test, we numerically integrated the motion of test particles in a circular, circumbinary orbit around the binary system of Model 1. For orbits of radius 2.6 A.U. that are inclined by  $\approx 20^\circ$  relative to the plane of the binary, the line of nodes regresses at  $6.3 \times 10^{-3} \text{ rad year}^{-1}$ , corresponding to  $40 \text{ m s}^{-1}$ . The projection of this velocity normal to the plane of the binary is  $14 \text{ m s}^{-1}$ , consistent with the screen speed of the model. Furthermore, given the mass ratio and eccentricity of the binary, test particles at 2.6 A.U. are long-term dynamically stable against ejection (Holman & Wiegert 1999).

One difference between the model and observed light curve from 2001-02 (Figure 4) is that the start of ingress, and end of egress, are too abrupt in the model. This is probably due to the assumption of a perfectly sharp and straight edge. Any small scale structure or optically thin border would soften the shoulders of the light curve. Likewise, we did not attempt to model temporal variations in the scattered light during eclipses, which could be due to the spatial distribution of dust in the plane of the binary, or ahead of the occulting edge.

There is conflicting evidence regarding star B’s luminosity. Kearns & Herbst (1998) found that during a few of the earliest observed re-brightenings, the system exceeded its uneclipsed flux, implying  $L_B/L_A > 1$ . On the other hand, JW03 reported 0.67 mag eclipses at a time when the total eclipses of star B were being diluted by flux from star A, suggesting  $L_B/L_A = 0.85$ . In this work we adopted  $L_B/L_A = 1$ , recognizing that intrinsic variability of PMS stars is common, and may be responsible for the confusion.

Predictions for the full radial velocity curve are given in Figure 5. They are subject to the uncertainty in the total stellar mass, and also the reliability of the two H02 measurements,

which may be contaminated by scattered light. Outside eclipses the peak-to-peak variations are  $\approx 10 \text{ km s}^{-1}$ . The largest variations occur during eclipses, when the star's photosphere is hidden. Still, it may be possible to measure the radial velocity variation during eclipses if the stars carry an extended envelope of gas (Deming, Charbonneau, & Harrington 2003).

We can also predict the results of additional archival studies and future monitoring campaigns. Prior to about 1960, no photometric variations were seen, apart from any intrinsic variations of the stars. The eclipse duration grew between 1970 and 1985, at which point the light curve became more complex due to eclipses of both stars. In the future the eclipse duration will continue to grow, and by about 2012 the system will be completely covered. When the system will come back into view depends on the unknown extent of the obscuring screen.

It is a pleasure to acknowledge helpful discussions with Dimitar Sasselov, Martin Winn, Marc Kuchner, Scott Gaudi, and Lucas Laursen. We are also very grateful to Bill Herbst and Catrina Hamilton for providing the 2001-02 light curve. This work was supported by the National Science Foundation under Grant No. 0104347.

## REFERENCES

- Agol, E., Barth, A.J., Wolf, S., & Charbonneau, D. 2003, preprint [astro-ph/0309309]
- Barge, P. & Viton, M. 2003, ApJL, 593, L117
- Deming, D., Charbonneau, D., & Harrington, J. 2003, preprint [astro-ph/0311608]
- Grinin, V.P. & Tambovtseva, L.V. 2002, Ast. Lett. 28, 601
- Hamilton, C.M., Herbst, W., Shih, C., & Ferro, A.J. 2001, ApJ, 554, L201
- Hamilton, C.M., Herbst, W., Mundt, R., Bailer-Jones, C.A.L., & Johns-Krull, C.M. 2003, ApJL, 591, L45
- Herbst, W. et al. 2002, PASP, 114, 1167 [H02]
- Holman, M. & Wiegert, C. 1999, AJ, 117, 621
- Johnson, J. & Winn, J.N. 2003, preprint [astro-ph/0312428; JW03]
- Kearns, K.E. & Herbst, W.H. 1998, AJ, 116, 261

Winn, J.N., Garnavich, P.M., Stanek, K.Z., & Sasselov, D.D. 2003, *ApJL*, 593, L121

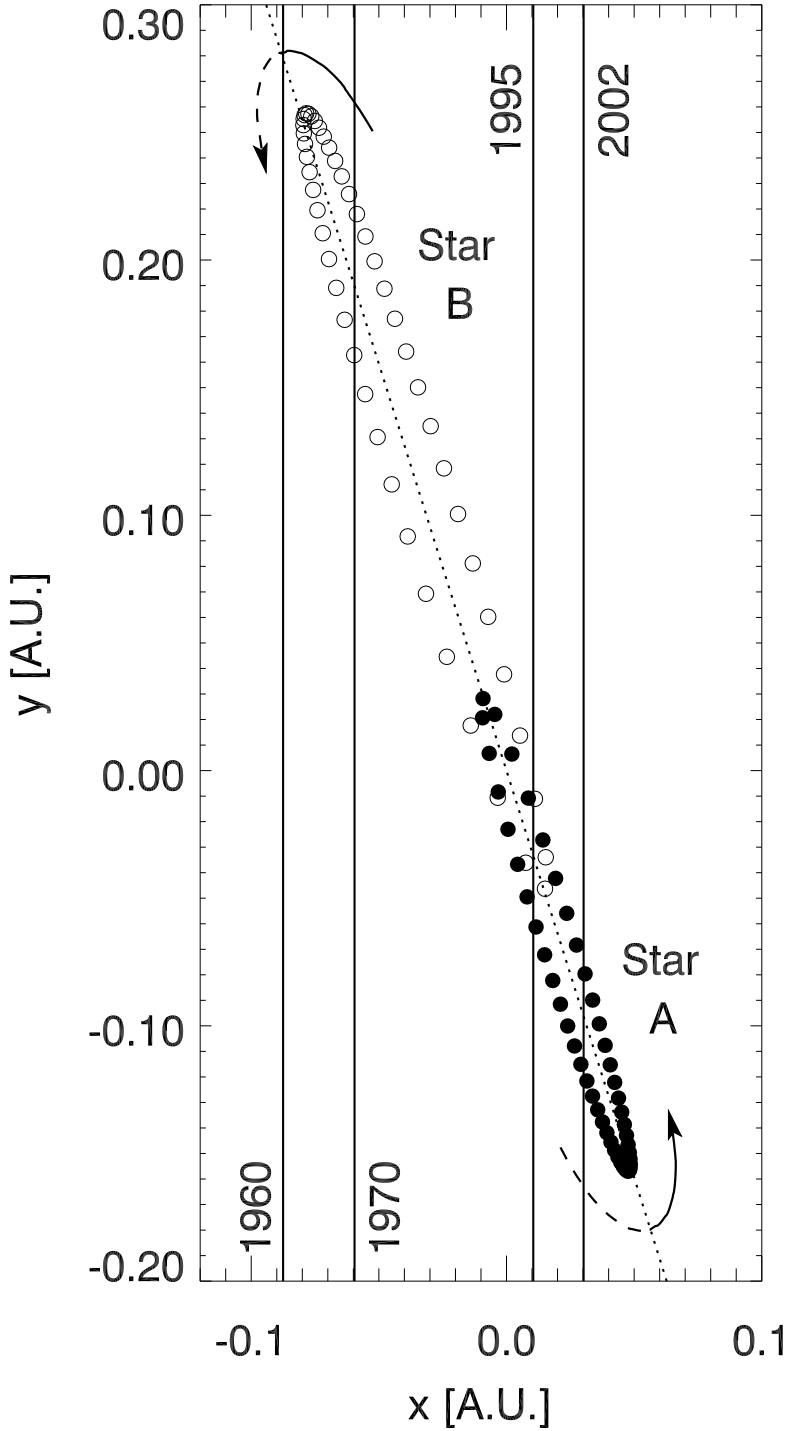


Fig. 1.— Projected binary orbit of Model 1. The center of mass defines the origin, and the  $z$ -axis points towards the observer. The positions of stars A and B are plotted with a time sampling  $P/50$ . The dashed line is the line of nodes, and the arrows show the motion of the stars as they move between  $z > 0$  (solid) and  $z < 0$  (dashed). Vertical lines indicate the location of the edge of the obscuring screen at some years of interest. The screen moves from left to right, blocking the stars whenever they are to the left of the edge.

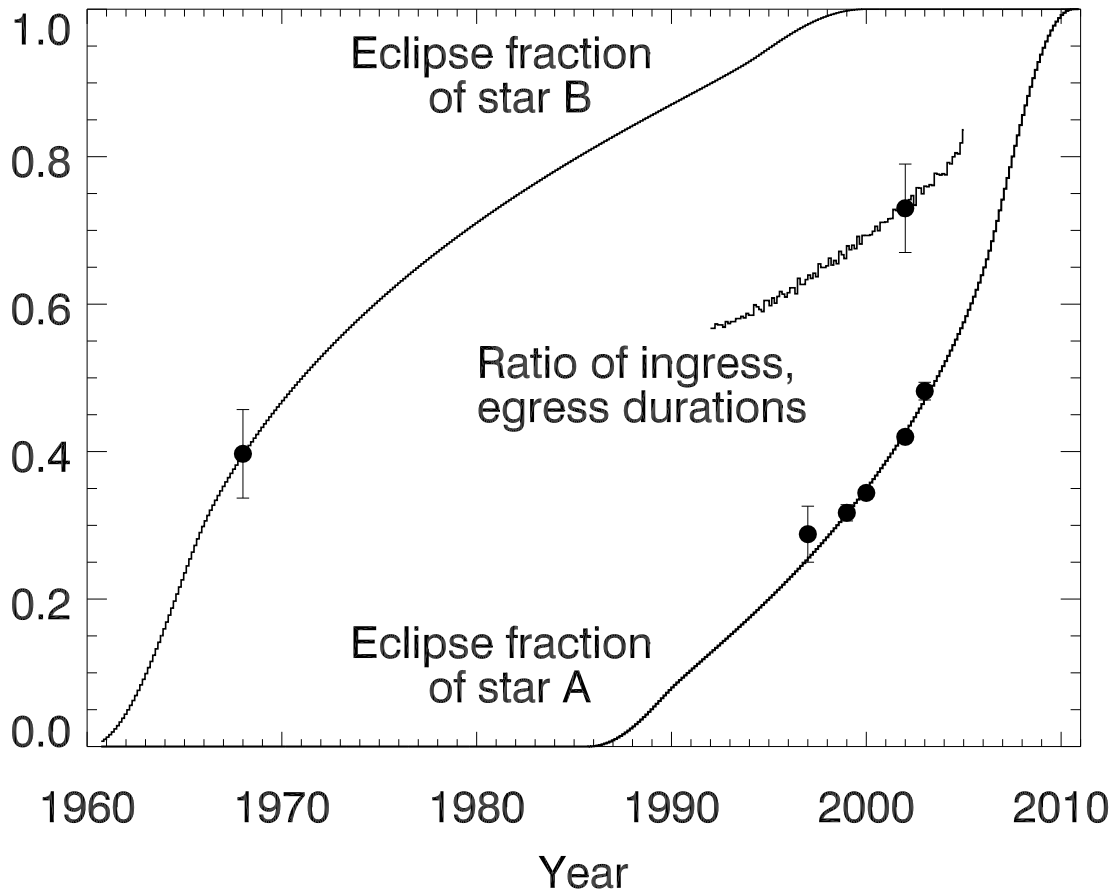


Fig. 2.— Time evolution of the eclipse fractions of stars A and B, and the ratio of ingress and egress durations of star A, for the best-fit model. The solid circles are observed values, listed in Table 1.

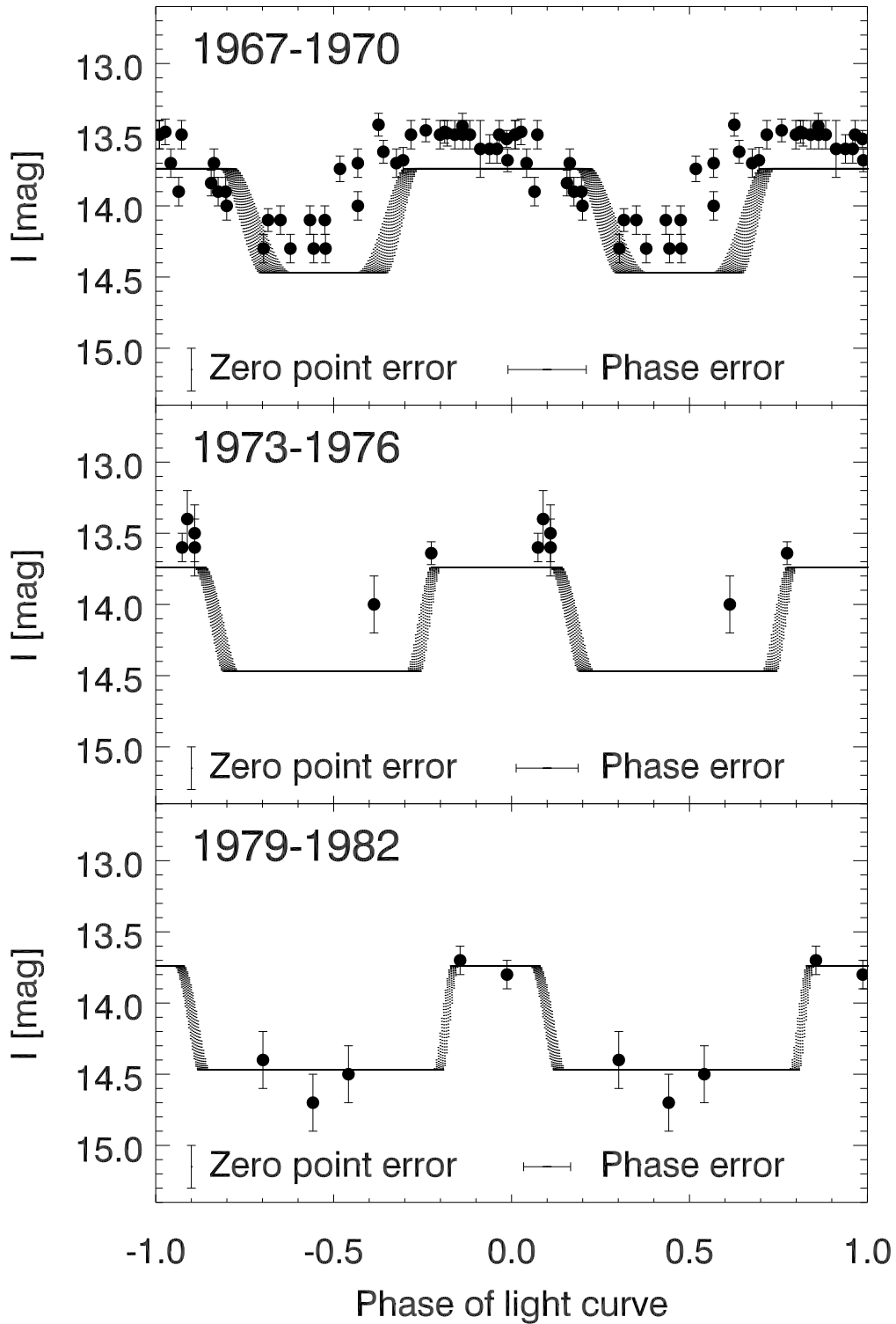


Fig. 3.— Comparison of phased light curves from the model (dotted lines) and data from Asiago Observatory (solid circles). The light curves were phased with the H02 ephemeris. The thickness of the model light curves during ingress and egress is due to the growth in eclipse duration during the 3-year time spans.

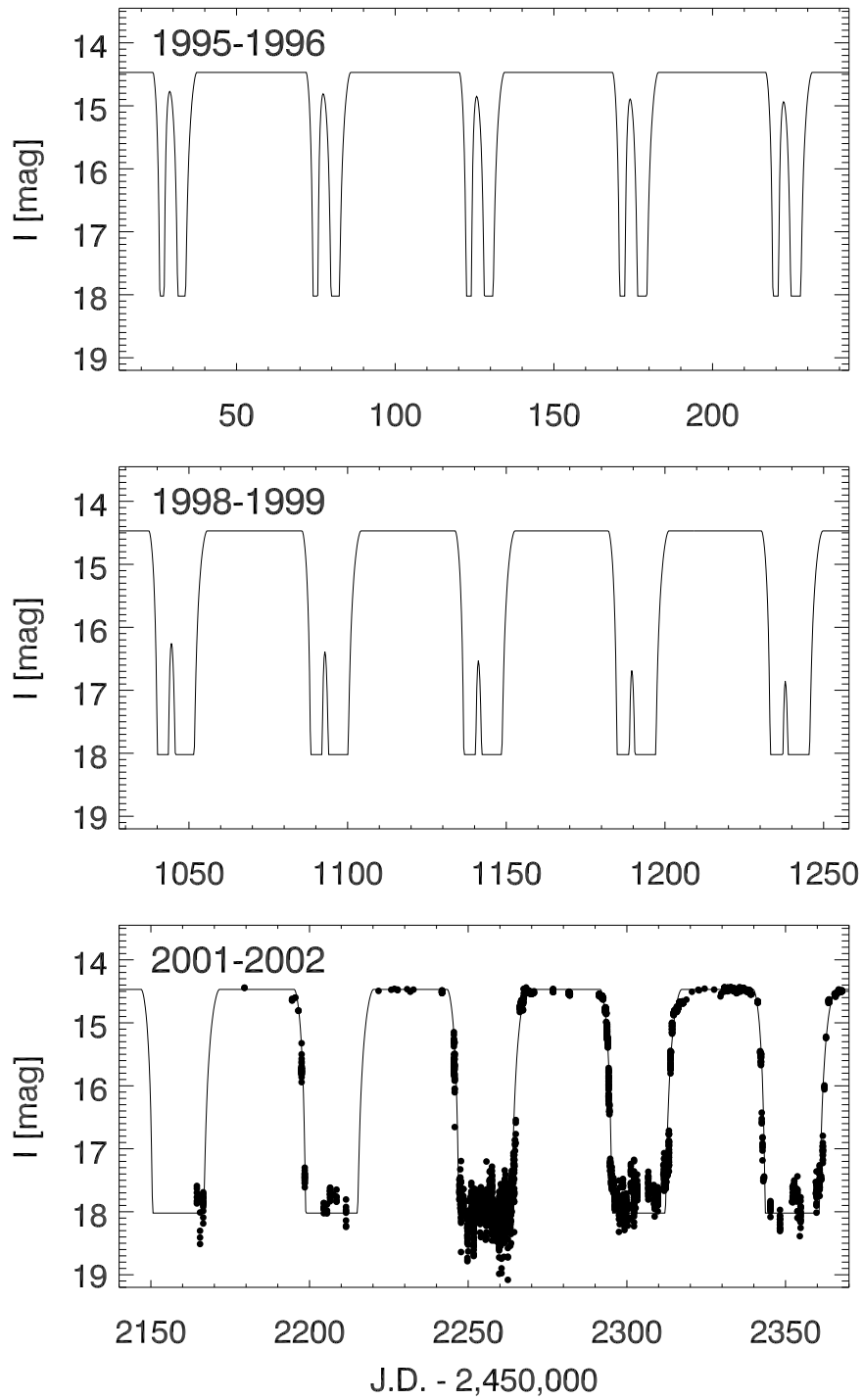


Fig. 4.— Model light curves from three recent time periods. The top and middle panels show the gradual diminution of the amplitude of the re-brightening events. The bottom panel compares the model light curve and the H02 light curve.

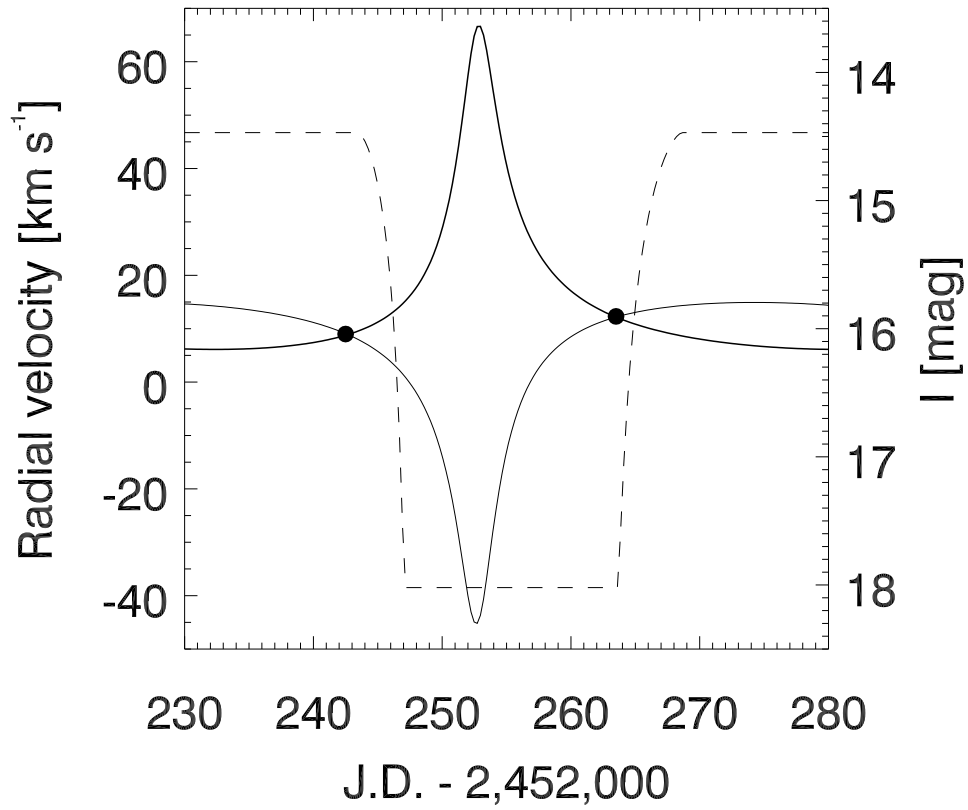


Fig. 5.— Two possible solutions for the radial velocity variation of star A (solid lines, left-hand axis). Positive velocity corresponds to motion away from the Sun. Model 1 corresponds to the positive radial velocity peak, and model 2 corresponds to the negative peak. Also plotted is the corresponding  $I$  magnitude of the model light curve (dashed line, right-hand axis). Solid circles are measurements by Hamilton et al. (2003).

Table 1. Model constraints

| Quantity                      | Star | Year   | Value <sup>a</sup> |
|-------------------------------|------|--------|--------------------|
| Eclipse fraction <sup>b</sup> | B    | 1968.0 | $0.397 \pm 0.060$  |
| Eclipse fraction <sup>b</sup> | A    | 1997.0 | $0.288 \pm 0.038$  |
| Eclipse fraction <sup>b</sup> | A    | 1999.0 | $0.317 \pm 0.011$  |
| Eclipse fraction <sup>b</sup> | A    | 2000.0 | $0.344 \pm 0.008$  |
| Eclipse fraction <sup>b</sup> | A    | 2002.0 | $0.420 \pm 0.008$  |
| Eclipse fraction <sup>b</sup> | A    | 2003.0 | $0.482 \pm 0.012$  |
| Ingress duration <sup>c</sup> | A    | 2002.0 | $3.8 \pm 0.3$ days |
| Egress duration <sup>c</sup>  | A    | 2002.0 | $5.2 \pm 0.3$ days |

<sup>a</sup> All quantities and their uncertainties were estimated with pencil and ruler from the light curves of H02, JW03, and P. Garnavich (unpublished).

<sup>b</sup> Eclipse fraction is the fraction of the photometric period during which the total flux is below 52% of the maximum.

<sup>c</sup> Ingress and egress durations were estimated by measuring the time between the  $I = 14.6$  and  $17.6$  levels, and then multiplying by 1.33, to match our choice of limb-darkening model.

Table 2. Optimized model parameters

| Parameter   | Model 1       | Model 2       |
|---|---------------|---------------|
| Mass ratio, $M_B/M_A$   | 0.61          | 0.61          |
| Radius of star B [solar radii]  | 1.8           | 1.8           |
| Eccentricity, $e$   | 0.70          | 0.70          |
| Longitude of ascending node, <sup>b</sup> $\Omega$ [deg]                  | $-72^\circ.6$ | $105^\circ.9$ |
| Argument of pericenter, $\omega$ [deg]                                    | $-7^\circ.2$  | $184^\circ.9$ |
| Inclination, $i$ [deg]  | $84^\circ.6$  | $81^\circ.0$  |
| Heliocentric radial velocity of C.O.M. <sup>a</sup> [km s <sup>-1</sup> ] | +15.5         | +5.7          |
| Relative velocity of screen and C.O.M. [m s <sup>-1</sup> ]               | 13            | 13            |

<sup>a</sup> Positive velocity corresponds to motion away from the Sun.

<sup>b</sup> Measured counter-clockwise, relative to the  $x$ -axis, as in Figure 1. The orientation of the occulting edge in celestial coordinates is unknown.